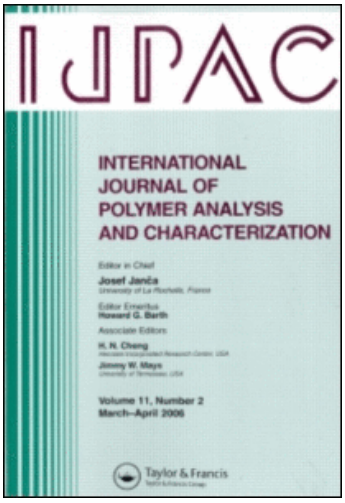

International Journal of Polymer Analysis and Characterization
Publication details, including instructions for authors and subscription information:
http://www.informaworld.com/smpp/title~content=t713646643

Tensile and Fracture Behaviors of PET/PTT Side-Side Bicomponent Filament

Si-Hai Chen[a]; Shan-Yuan Wang[a]
[a] Key Laboratory of Textile Materials of Ministry of Education, Donghua University, Shanghai, China

Online publication date: 16 April 2010

To cite this Article Chen, Si-Hai and Wang, Shan-Yuan(2010) 'Tensile and Fracture Behaviors of PET/PTT Side-Side Bicomponent Filament', International Journal of Polymer Analysis and Characterization, 15: 3, 147 — 154
To link to this Article: DOI: 10.1080/10236660903585350
URL: http://dx.doi.org/10.1080/10236660903585350

International Journal of Polymer Anal. Charact., 15: 147–154, 2010

ISSN: 1023-666X print
DOI: 10.1080/10236660903585350

Taylor & Francis
Taylor & Francis Group

TENSILE AND FRACTURE BEHAVIORS OF PET/PTT SIDE-SIDE BICOMPONENT FILAMENT

Si-Hai Chen and Shan-Yuan Wang
Key Laboratory of Textile Materials of Ministry of Education, Donghua University, Shanghai, China

In this work, the tensile and fracture behaviors of PET/PTT side-side bicomponent filament are investigated by comparisons to single-component PTT and PET counterparts. Some unique tensile behaviors of PET/PTT are attributed to its spring-like curliness and low initial modulus of the PTT side. Tensile stress of PET/PTT is between that of PTT and PET in real extension region. The shape of "hysteresis" loops of PET/PTT looks like the combination of that of PTT and PET. The decay rates of loop width are measured, and loop numbers for PET, PTT, and PET/PTT needed to reach stable shape are predicted. We also use SEM to explore the fracture behaviors of PET/PTT by relating to those of PTT and PET. Some unique fracture behaviors of PET/PTT are found.

Keywords: Bicomponent filament; Counterpart; Fracture; Hysteresis; Tensile

INTRODUCTION

Poly(trimethylene terephthalate) (3GT or PTT) has received much attention as a polymer for use in textiles, packaging, flooring, and other end uses.[1,2] In the fiber industry, it is also used in PET/PTT bicomponent filament, composed of poly(ethylene terephthalate) (2GT or PET) and PTT with suitable volume ratio and proper geometric arrangement, which possesses a helical self-crimp due to different shrinkage of the two components.[3,4] This self-crimp property offers the filaments, yarns, and fabrics a desirable stretch.

Much research[5–7] has been conducted on tensile behaviors of PTT and PET filaments, whereas relatively less has been done on PET/PTT bicomponent filament. In this study, we mainly investigate tensile and fracture behaviors of PET/PTT side-side by comparisons to single-component PTT and PET, which can imitate basic mechanical properties of PET and PTT counterparts in PET/PTT, with the

Submitted 24 November 2009; accepted 30 December 2009.
The authors would like to give sincere thanks to Mr. X. Chen and Mr. S. H. Jia for supporting the instruments and unremitting help in measurement work, and to the anonymous reviewers for their valuable comments and suggestions.

Correspondence: Si-Hai Chen, Key Laboratory of Textile Materials of Ministry of Education, Department of Textile Materials and Design, Donghua University, No. 2999 North Renmin Rd., Songjiang, Shanghai 201620, China. E-mail: sihaic@gmail.com

aim to explore some distinct properties of PET/PTT by relating to the individual properties of PTT and PET models.

EXPERIMENTAL SECTION

Materials

PTT/PET side-side of 50/50 volume ratio with a linear density of 22 tex (1 tex = 1 g/km) is made by conjugated melt spinning fiber-grade pellets of PTT and PET and drawing it on a two-stage frame. PTT and PET filaments of 22 tex are made by melt spinning using the same pellets that PET/PTT is made from, and drawing and processing under the same conditions as PTT/PET. The drawing and processing conditions of PET and PTT filaments are determined such that they experienced almost identical mechanical and thermal history and can basically represent the individual counterparts in the PET/PTT filament. Tensile properties of resulting filaments are presented in Figure 1.

Measurements

A YG061 electronic dynamometer was used to perform tensile measurements. For one-time stretch to rupture tests, a gauge length of 250 mm, an extension rate of 500 mm/min, and a pre-tension of 0.02 cN/tex (1 cN/tex = 0.01 N/tex) were applied. For multi-cycle tensile tests, the setting elongations of 15% for both PET and PTT

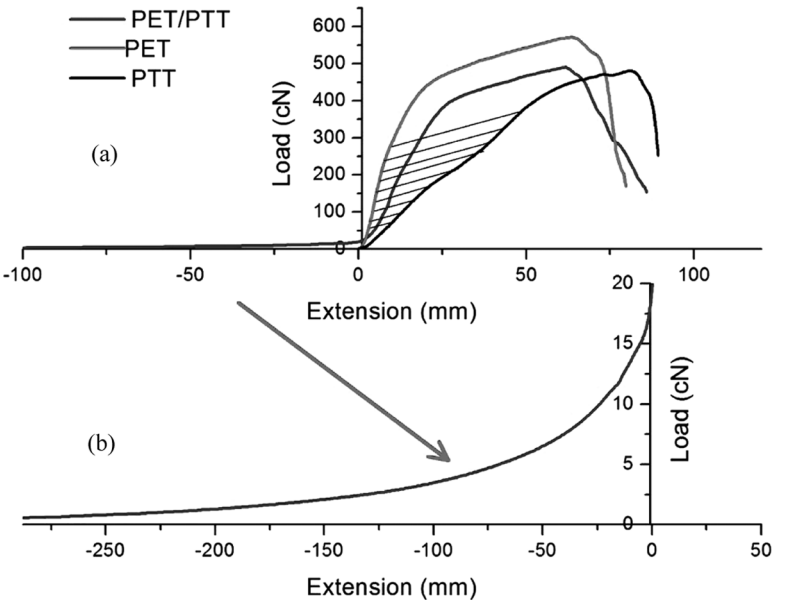

Figure 1. Comparisons of tensile behavior of PET/PTT with PET and PTT model filaments: (a) the real extension region of individual filaments, and (b) the de-crimping region and part of the mixing region of de-crimping and real extension of PET/PTT filament.

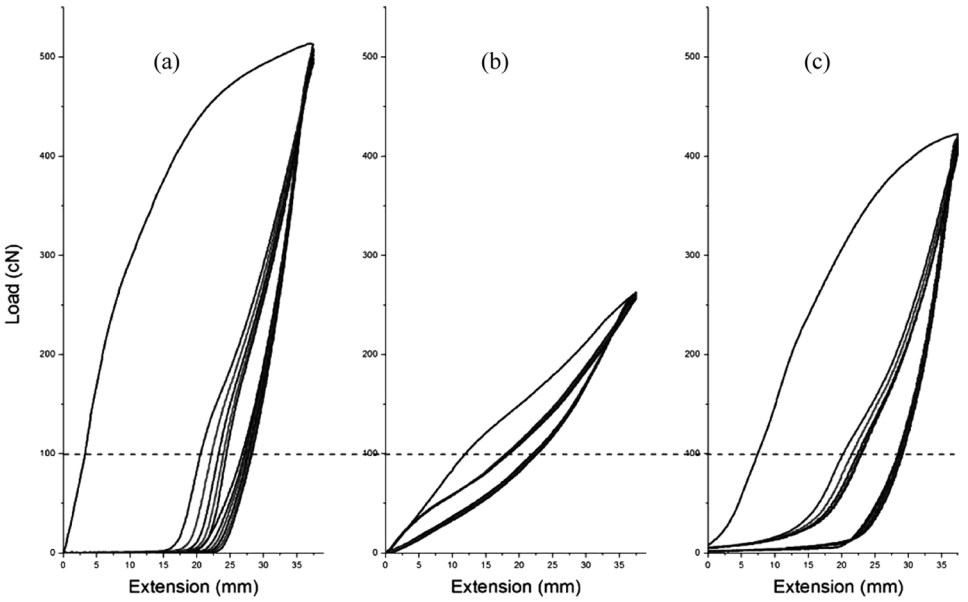

Figure 2. "Hysteresis" loops of multi-cycle tensile and recovery for (a) PET of 15% elongation, (b) PTT of 15% elongation, and (c) PET/PTT filament of 125% elongation at pre-tension of 0.02 cN/tex.

and 125% for PET/PTT, a gauge length of 250 mm, and pre-tension of 0.02 cN/tex with an extension rate of 500 mm/min were applied. The results used are the averages of 10 measurements for each specific item. All tests were performed at room temperature of 25°C and relative humidity of 65%. The results were calculated according to:

$$W(n) = E_u(n) - E_l(n) \tag{1}$$

where W(n) is the width of the n-th loop, and $E_l(n)$ and $E_u(n)$ are the extensions of the n-th load and unload cycle at load of 100 cN (1 cN = 0.01 N), respectively, in Figure 2. For the overlapping of the curves and the error of W(n) increase with number of loops, the width of the first five loops are given in Table I. These data are fitted by a nonlinear equation (exponential decay):

$$W(n) = W_0 + A * \exp(-K_0 * n) \tag{2}$$

Table I. Experimental data of first five loop widths at load of 100 cN used for nonlinear curve fitting

Samples	W(1)	W(2)	W(3)	W(4)	W(5)
PET	7.78	5.68	5.07	4.57	4.50
PTT	4.76	4.45	4.23	4.05	3.88
PET/PTT	8.49	7.38	6.83	6.49	6.31

W(n) is the width of the n-th loop. Unit: mm.

where W_0 is the asymptotic value of the loop width, A is the amplitude of the decay of the loop width, and K_0 is the rate of decay of the loop width.

The ruptured fibers were collected and labeled separately for SEM observations. SEM photographs were taken on a DXS-10A scanning electron microscope. The magnification used was 3000.

RESULTS AND DISCUSSION

Tensile Behavior

The one-time extension to rupture behavior of PTT, PET, and PET/PTT filaments is illustrated in Figure 1. The differences are more obvious in the low force region as shown in Figure 1(b). This is mainly composed of the de-crimping region and part of the mixing region of the de-crimping and real extension regions. In the real extension region in Figure 1(a), the curve of PET/PTT filament is almost positioned in the silhouetted area between the curves of PET and PTT model filaments, and seems to resemble more the shape of PET. From the characteristics of the curves, it can be said that the tenacity and initial modulus of PET/PTT are ranked in the order PET > PET/PTT > PTT, and it can also be inferred that in the broken sequence of PET/PTT the PTT side breaks later than the PET side, although the delay of break of the PTT side is too short to be observed by applying the usual methods.

The elongations to break of all the filaments are less than 30%, if the whole elongation is carried out in the real extension region. The maximum elongation of PET/PTT could reach 150% under the pre-tension of 0.02 cN/tex, and this is unique for PET/PTT filament.

Multi-Cycle Tensile Behavior

A fibrous material property can be classified as "perfect elasticity," "complete elasticity," or "imperfect elasticity" according to the shape of "hysteresis" loops from its multi-cycle tensile responses.[8] By comparisons in Figure 2, PTT, PET, and PET/PTT filaments all manifest a certain "hysteresis." In the range of measurement, the curve shape of PTT is analogous to "complete elasticity," PET clearly has "imperfect elasticity," and PET/PTT seems to be located between "complete elasticity" and "imperfect elasticity." PTT recovers almost completely but via a different path from the load curve, forming narrow and tilted "hysteresis" loops concentrated together; PET only partly recovers, and formed loops are wider and more vertical. Both the deviations of load and unload curves of PET are greater than those of PTT. The curve shape of PET/PTT looks like a mixing of that of PTT and PET, with its lower force region close to PTT and the higher close to PET, and the loops are narrow and hook-shaped. The "hysteresis" loops in the low force region can be attributed to the formation of the helical crimp of PET/PTT caused by longitudinally bilateral different shrinkage of PET and PTT and low initial modulus of PTT in the mixing region of de-crimping and real extension.[9,10]

The variation of W(n), depicted in Equation (1), is used to characterize the relaxation behavior and the maintenance of the loop shape of these filaments under

Table II. Specifications of nonlinear curve fitting

Filament	Fitting parameters	Value	Standard error
PET	W_0 (mm)	4.42409	0.11439
	A (mm)	8.45666	0.85864
	K_0	−0.92758	0.11141
PTT	W_0 (mm)	3.27398	0.14422
	A (mm)	1.84293	0.11592
	K_0	−0.22037	0.03233
PET/PTT	W_0 (mm)	6.11274	0.03714
	A (mm)	4.38044	0.08006
	K_0	−0.61302	0.02509

multi-cycle stretch. The experimental data of W(n) for the first five cycles for three filaments are presented in Table I. These data are fitted by nonlinear (exponential decay) Equation (2) and the specifications and results are illustrated in Table II. From Figure 3, we can see the rate of width decay, K_0, of PET/PTT, which is ranked as PET > PET/PTT > PTT, and the number of cycles for PET, PTT, and PET/PTT "hysteresis" loop needed to reach relatively stable shape ($W - W_0/A < 0.0001$): 10 loops for PET, 16 loops for PET/PTT, and 42 loops for PTT. This means that both the loading and unloading path keep almost unchanged, reflecting that a relatively stable tensile behavior is reached. PTT has an antifatigue property that is superior to that of PET/PTT and PET in the region of the performed measurements.[2]

Fracture Behavior

The typical fracture behavior of PTT, PET, and PET/PTT filaments under constant deformation rate of 200%/min is presented in Figure 4. These fractures

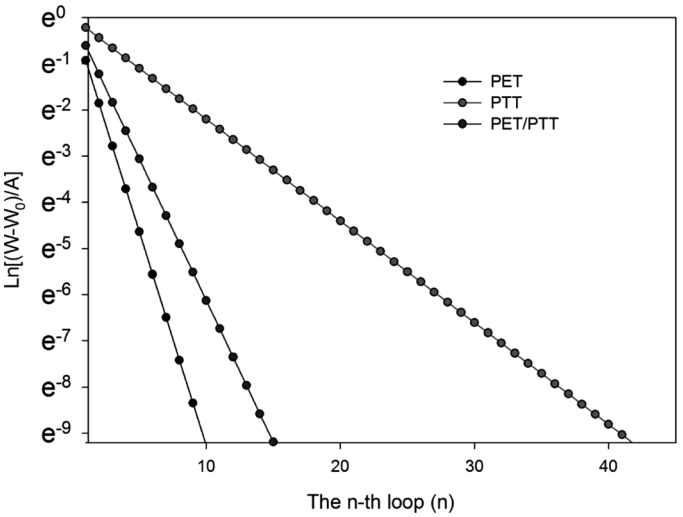

Figure 3. Plot of ln-[(W−W_0)/A] vs. "n" and extrapolation to intersect with abscissa axis.

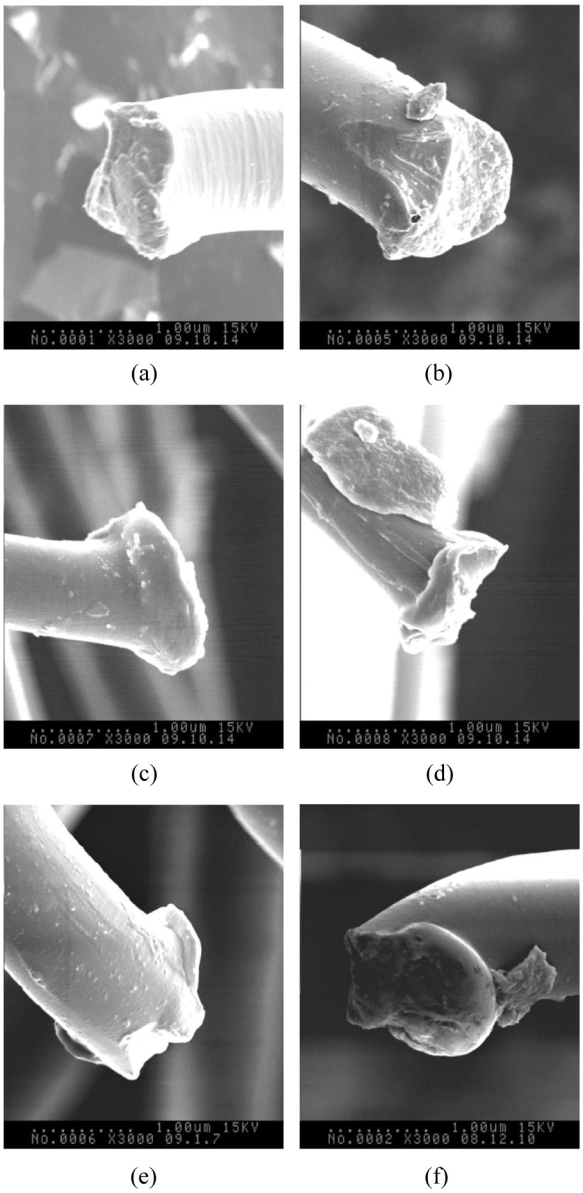

Figure 4. Tensile fracture behavior of PET, PTT, and PET/PTT filaments: (a) V-notch on PET, (b) striations and slightly enlarged head on PET, (c) significantly enlarged head on PTT, (d) collapsed circumference on PTT, (e) V-notch on PET/PTT, and (f) collapsed circumference on PET/PET.

seem all to belong to the ductile type.[11,12] PET has a clear V-notch, some striations perpendicular to the fiber axis, and a slightly enlarged diameter of the broken head in Figures 1(a) and (b); PTT has a significantly enlarged head with the circumference collapsed outward and no clear V-notch and traverse striation as seen in

Figures 1(c) and (d). These differences may be attributed to the higher recovery of PTT, which snaps back much faster than PET does. The fracture of PET/PTT looks like a combination of the characteristics of PTT and PET from two individual sides in Figures 1(e) and (f). If we assume that fracture initiates at V-notch and striations belonging to the PET side, then PTT always occupies the inner side of a coil, whereas PET occupies the outer one, and the cracks of PET/PTT should begin at the PET side, which implies that the PTT side is broken later. This is coincident with the case depicted in Figure 1. No clear split along the interface of PET/PTT is observed, manifesting good adhesion of the interface between the PET and PTT sides.

CONCLUSIONS

By comparing PET/PTT with PTT and PET model filaments, the ranking of tenacity is in the order PET > PET/PTT > PTT in all of the real extension regions. The low force de-crimping region is the main cause of the high stretching and accounts for more than 70% of the total extension of PET/PTT.

The narrow and hook-shaped "hysteresis" loops in the low force region are mainly associated with the formation of the helical crimp of PET/PTT and to the low initial modulus of PTT. The rate of width decay with loop number is ranked as PET > PET/PTT > PTT, whereas the ability to maintain the loop shape is inversely ordered. The predicted number of loops to reach relatively stable shape is 10, 16, and 42 for PET, PET/PTT, and PTT, respectively.

SEM analyses show that a combined fracture behavior of individual sides of PTT and PET is the dominant characteristic for PET/PTT filament, that the broken surface of PET/PTT supporting PTT side is broken later, and that no splitting along the interface of PET/PTT is observed.

REFERENCES

1. Hwo, C., H. Brown, P. Casey, H. Chuah, K. Dangayach, T. Forschner, M. Moerman, and L. Oliveri. 2000. Opportunities of Corterra PTT fibers in textiles. *Chem. Fibers Int.* 50: 53–56.
2. Chuah, H. H. 2003. In *Encyclopedia of Polymer Science and Technology*, 3rd ed., vol. 3, pp. 544–557. New York: John Wiley.
3. Rwei, S. P., Y. T. Lin, and Y. Y. Su. 2005. Study of self-crimp polyester fibers. *Polym. Eng. Sci.* 45: 838–445.
4. Oh, T. H. J. 2006. Effects of spinning and drawing conditions on the crimp contraction of side-by-side poly(trimethylene terephthalate) bicomponent fibers. *J. Appl. Polym. Sci.* 102: 1322–1324.
5. Ward, I. M., and M. A. Wilding. 1976. The mechanical properties and structure of poly(m-methylene terephthalate) fibers. *J. Polym. Sci. Polym. Phys.* 14: 263–274.
6. Chen, K. Q., and X. Z. Tang. 2004. Instantaneous elastic recovery of poly(trimethylene terephthalate) filament. *J. Appl. Polym. Sci.* 91: 1976–1975.
7. Houck, M. M., R. A. Huff, P. C. Lowe, and R. E. Menold. 2001. Poly(trimethylene terephthalate): A "new" type of polyester fiber. *Forensic Sci. Commun.* 3: 3.
8. Adanur, S. 1995. *Wellington Sears Handbook of Industrial Textiles*. Lancaster, Penn.: Technomic Pub., pp. 579–582.

9. Burte, H. M. 1954. The detection of modification in animal fibers: II. Tensile recovery at 65% R. H. *Text. Res. J* 24: 414.
10. Frank, F. 1960. Some load-extension properties of crimped fibers. *J. Text. Inst.* 51: T83–T90.
11. Nissen, K. E., B. H. Stuart, M. G. Stevens, and A. T. Baker. 2008. The tensile and tear properties of a biodegradable polyester film. *Int. J. Polym. Anal. Charact.* 13: 190–199.
12. Hearle, J. W. S., B. Lomas, and W. D. Cooke. 1998. *Atlas of Fibre Fracture and Damage to Textiles*, 2nd ed. Cambridge: Woodhead, pp. 42–49.